PROCEEDINGS OF SCIENCE

Gauge-Higgs unification at e^+e^- linear colliders

Yutaka Hosotani*
Department of Physics, Osaka University
Toyonaka, Osaka 560-0043, Japan
E-mail: hosotani@het.phys.sci.osaka-u.ac.jp

In gauge-Higgs unification the 4D Higgs boson appears as a part of the fifth dimensional component of gauge potentials, namely as a fluctuation mode of the Aharonov-Bohm phase in the extra dimension. The $SO(5)\times U(1)\times SU(3)$ gauge-Higgs unification gives nearly the same phenomenology as the standard model (SM) at low energies. It predicts KK excited states of photon, Z boson, and Z_R boson (Z' bosons) around 7 - 8 TeV. Quarks and leptons couple to these Z' bosons with large parity violation, which leads to distinct interference effects in $e^+e^-\to\mu^+\mu^-, q\bar{q}$ processes. At 250 GeV ILC with polarized electron beams, deviation from SM can be seen at the 3 - 5 sigma level even with 250 fb^{-1} data, namely in the early stage of ILC. Signals become stronger at higher energies. Precision measurements of interference effects at electron-positron colliders at energies above 250 GeV become very important to explore physics beyond the standard model.

Corfu Summer Institute 2018 "School and Workshops on Elementary Particle Physics and Gravity" (CORFU2018)
31 August - 28 September, 2018
Corfu, Greece

*Speaker.

PoS(CORFU2018)075

1. Gauge-Higgs unification

The existence of the Higgs boson of a mass 125 GeV has been firmly confirmed. It establishes the unification scenario of electromagnetic and weak forces. In the standard model (SM) electromagnetic and weak forces are unified as $SU(2)_L \times U(1)_Y$ gauge forces. The $SU(2)_L \times U(1)_Y$ gauge symmetry is spontaneously broken by the Higgs scalar fields, whose neutral component appears as the observed Higgs boson. Although almost all experimental data are consistent with the SM, it is not clear whether the observed Higgs boson is precisely what the SM assumes to exit.

The gauge sector of the SM is beautiful. The gauge principle dictates how quarks and leptons interact with each other by gauge forces. In the SM the Higgs field gives masses to quarks, leptons, and weak bosons. However, the potential for the Higgs boson must be prepared by hand such that it induces the spontaneous breaking of $SU(2)_L \times U(1)_Y$ symmetry. To put it differently, there is no principle for the Higgs field which determines how the Higgs boson interacts with itself and other fields. The lack of a principle results in the arbitrariness in the choice of parameters in the theory. Furthermore the Higgs boson acquires an infinitely large correction to its mass at the quantum level which must be cancelled by fine tuning of bare parameters. It is called as the gauge hierarchy problem. In addition, even the ground state for the Higgs boson may become unstable against quantum corrections.

Gauge-Higgs unification (GHU) naturally solves those problems. The 4d Higgs boson appears as a fluctuation mode of an Aharonov-Bohm (AB) phase in the fifth dimension of spacetime, thus becoming a part of gauge fields. By dynamics of the AB phase the Higgs boson acquires a finite mass at the quantum level, which is protected from divergence by the gauge principle. The interactions of the Higgs boson are governed by the gauge principle, too. In short, gauge fields and the Higgs boson are unified.[1]-[3]

A realistic model of gauge-Higgs unification has been proposed. It is the $SO(5) \times U(1)_X \times SU(3)_C$ gauge-Higgs unification in the Randall-Sundrum warped space. It reproduces the SM content of gauge fields and matter content, and SM phenomenology at low energies. It leads to small deviations in the Higgs couplings. It also predicts new particles at the scale 5 TeV to 10 TeV as Kaluza-Klein (KK) excitation modes in the fifth dimensions. Signals of these new particles can be seen both at LHC and at ILC.[4]-[13]

One of the distinct features of the gauge-Higgs unification is large parity violation in the couplings of quarks and leptons to KK exited states of gauge bosons. Right-handed quarks and leptons have much larger couplings to the first KK excited states of photon, Z boson, and Z_R boson (called as Z' bosons) than the left-handed ones. These Z' bosons have masses around 7 TeV - 8 TeV. We will show below that even at 250 GeV ILC with 250 fb^{-1} data large deviations from the SM in various cross sections in $e^+e^- \to f\bar{f}$ processes can be seen by measuring the dependence on the polarization of the electron beam. The key technique is to see interference effects between the contribution from photon and Z boson and the contribution from Z' bosons.

We comment that there might be variation in the matter content of the $SO(5) \times U(1)_X \times SU(3)_C$ gauge-Higgs unification. Recently a new way of introducing quark and lepton multiplets has been found, which can be embedded in the $SO(11)$ gauge-Higgs grand unification.[13] Other options for fermion content have been proposed.[12] These models can be clearly distinguished from each other by investigating the polarization dependence of electron/positron beams in fermion pair pro-

duction at ILC. Note also that gauge-Higgs unification scenario provides new approaches to dark matter, Higgs, and neutrino physics.[14]-[18]

2. $SO(5)\times U(1)\times SU(3)$ GHU in Randall-Sundrum warped space

The theory is defined in the Randall-Sundrum (RS) warped space whose metric is given by

$$ds^2 = e^{-2\sigma(y)}\eta_{\mu\nu}dx^\mu dx^\nu + dy^2, \tag{2.1}$$

where $\mu,\nu = 0,1,2,3$, $\eta_{\mu\nu} = \mathrm{diag}(-1,+1,+1,+1)$, $\sigma(y) = \sigma(y+2L) = \sigma(-y)$, and $\sigma(y) = ky$ for $0 \le y \le L$. It has the topological structure S^1/Z_2. In terms of the conformal coordinate $z = e^{ky}$ ($1 \le z \le z_L = e^{kL}$) in the region $0 \le y \le L$

$$ds^2 = \frac{1}{z^2}\left(\eta_{\mu\nu}dx^\mu dx^\nu + \frac{dz^2}{k^2}\right). \tag{2.2}$$

The bulk region $0 < y < L$ ($1 < z < z_L$) is anti-de Sitter (AdS) spacetime with a cosmological constant $\Lambda = -6k^2$, which is sandwiched by the UV brane at $y = 0$ ($z = 1$) and the IR brane at $y = L$ ($z = z_L$). The KK mass scale is $m_{\rm KK} = \pi k/(z_L - 1) \simeq \pi k z_L^{-1}$ for $z_L \gg 1$.

Gauge fields $A_M^{SO(5)}$, $A_M^{U(1)_X}$ and $A_M^{SU(3)_C}$ of $SO(5)\times U(1)_X \times SU(3)_C$, with gauge couplings g_A, g_B and g_C, satisfy the orbifold conditions[7, 8, 13]

$$\begin{pmatrix} A_\mu \\ A_y \end{pmatrix}(x, y_j - y) = P_j \begin{pmatrix} A_\mu \\ -A_y \end{pmatrix}(x, y_j + y) P_j^{-1} \tag{2.3}$$

where $(y_0, y_1) = (0, L)$. For $A_M^{SO(5)}$

$$P_0 = P_1 = P_{\mathbf{5}}^{SO(5)} = \mathrm{diag}(I_4, -I_1)\ , \tag{2.4}$$

whereas $P_0 = P_1 = I$ for $A_M^{U(1)_X}$ and $A_M^{SU(3)_C}$. With this set of boundary conditions $SO(5)$ gauge symmetry is broken to $SO(4) \simeq SU(2)_L \times SU(2)_R$. At this stage there appear zero modes of 4D gauge fields in $SU(3)_C$, $SU(2)_L \times SU(2)_R$ and $U(1)_X$. There appear zero modes in the $SO(5)/SO(4)$ part of $A_y^{SO(5)}$, which constitute an $SU(2)_L$ doublet and become 4D Higgs fields. As a part of gauge fields the 4D Higgs boson $H(x)$ appears as an AB phase in the fifth dimension;

$$\hat{W} = P\exp\left\{ig_A\int_{-L}^{L} dy A_y\right\}\cdot P_1 P_0 \sim \exp\left\{i\left(\theta_H + \frac{H(x)}{f_H}\right)2T^{(45)}\right\}\ , \tag{2.5}$$

where

$$f_H = \frac{2}{g_w}\sqrt{\frac{k}{L(z_L^2-1)}} \sim \frac{2\, m_{\rm KK}}{\pi g_w \sqrt{kL}}\ . \tag{2.6}$$

$g_w = g_A/\sqrt{L}$ is the 4D weak coupling. Gauge invariance implies that physics is periodic in θ_H with a period 2π.

A brane scalar field $\hat{\Phi}_{(1,2,2,\frac{1}{2})}(x)$ or $\hat{\Phi}_{(1,1,2,\frac{1}{2})}(x)$ is introduced on the UV brane where subscripts indicate the $SU(3)_C \times SU(2)_L \times SU(2)_R \times U(1)_X$ content. Nonvanishing $\langle\hat{\Phi}\rangle$ spontaneously breaks $SU(2)_R \times U(1)_X$ to $U(1)_Y$, resulting in the SM symmetry $SU(3)_C \times SU(2)_L \times U(1)_Y$.

Once the fermion content is specified, the effective potential $V_{\rm eff}(\theta_H)$ is evaluated. The location of the global minimum of $V_{\rm eff}(\theta_H)$ determines the value of θ_H. When $\theta_H \neq 0$, $SU(2)_L \times U(1)_Y$ symmetry is dynamically broken to $U(1)_{\rm EM}$. It is called the Hosotani mechanism.[1] The W boson mass is given by

$$m_W \sim \sqrt{\frac{k}{L}}\, z_L^{-1} \sin\theta_H \sim \frac{\sin\theta_H}{\pi\sqrt{kL}}\, m_{\rm KK}\ . \tag{2.7}$$

As typical values, for $\theta_H = 0.10$ and $z_L = 3.6\times 10^4$ one find $m_{\rm KK} = 8.1\,{\rm TeV}$ and $f_H = 2.5\,{\rm TeV}$. There appears natural little hierarchy in the weak scale (m_Z) and the KK scale ($m_{\rm KK}$).

Quark and lepton multiplets are introduced in the vector representation **5** of $SO(5)$. Further dark fermions are introduced in the spinor representation **4** of $SO(5)$. This model is called as the A-model, and has been investigated intensively so far.[8]-[11] Recently an alternative way of introducing matter has been found.[13] This model, called as the B-model, can be implemented in the $SO(11)$ gauge-Higgs grand unification.[19, 20, 21] The matter content of the two models is summarized in Table 1. In this talk phenomenological consequences of the A-model are presented.

Table 1: Matter fields. $SU(3)_C \times SO(5) \times U(1)_X$ content is shown. In the A-model only $SU(3)_C \times SO(4) \times U(1)_X$ symmetry is maintained on the UV brane so that the $SU(2)_L \times SU(2)_R$ content is shown for brane fields. In the B-model given in ref. [13] the full $SU(3)_C \times SO(5) \times U(1)_X$ invariance is preserved on the UV brane.

	A-model	B-model
quark	$(\mathbf{3},\mathbf{5})_{\frac{2}{3}}\ (\mathbf{3},\mathbf{5})_{-\frac{1}{3}}$	$(\mathbf{3},\mathbf{4})_{\frac{1}{6}}\ (\mathbf{3},\mathbf{1})^+_{-\frac{1}{3}}\ (\mathbf{3},\mathbf{1})^-_{-\frac{1}{3}}$
lepton	$(\mathbf{1},\mathbf{5})_0\ (\mathbf{1},\mathbf{5})_{-1}$	$(\mathbf{1},\mathbf{4})_{-\frac{1}{2}}$
dark fermion	$(\mathbf{1},\mathbf{4})_{\frac{1}{2}}$	$(\mathbf{3},\mathbf{4})_{\frac{1}{6}}\ (\mathbf{1},\mathbf{5})^+_0\ (\mathbf{1},\mathbf{5})^-_0$
brane fermion	$(\mathbf{3},[\mathbf{2},\mathbf{1}])_{\frac{7}{6},\frac{1}{6},-\frac{5}{6}}$ $(\mathbf{1},[\mathbf{2},\mathbf{1}])_{\frac{1}{2},-\frac{1}{2},-\frac{3}{2}}$	$(\mathbf{1},\mathbf{1})_0$
brane scalar	$(\mathbf{1},[\mathbf{1},\mathbf{2}])_{\frac{1}{2}}$	$(\mathbf{1},\mathbf{4})_{\frac{1}{2}}$
Sym. on UV brane	$SU(3)_C \times SO(4) \times U(1)_X$	$SU(3)_C \times SO(5) \times U(1)_X$

The correspondence between the SM in four dimensions and the gauge-Higgs unification in five dimensions is summarized as

$$\begin{array}{ccc} \text{SM} & & \text{GHU} \\ \displaystyle\int d^4x \Big\{ \mathscr{L}^{\rm gauge} + \mathscr{L}^{\rm Higgs}_{\rm kinetic} \Big\} & \Rightarrow & \displaystyle\int d^5x\sqrt{-g}\ \mathscr{L}^{\rm gauge}_{\rm 5d} \\ \displaystyle\int d^4x \Big\{ \mathscr{L}^{\rm fermion} + \mathscr{L}^{\rm Yukawa} \Big\} & \Rightarrow & \displaystyle\int d^5x\sqrt{-g}\ \mathscr{L}^{\rm fermion}_{\rm 5d} \\ \displaystyle -\int d^4x\ \mathscr{L}^{\rm Higgs}_{\rm potential} & \Rightarrow & \displaystyle\int d^4x\, V_{\rm eff}(\theta_H) \end{array} \tag{2.8}$$

In the SM, $\mathscr{L}^{\rm gauge}$, $\mathscr{L}^{\rm Higgs}_{\rm kinetic}$ and $\mathscr{L}^{\rm fermion}$ are governed by the gauge principle, but $\mathscr{L}^{\rm Yukawa}$ and $\mathscr{L}^{\rm Higgs}_{\rm potential}$ are not. On the GHU side in (2.8), $\mathscr{L}^{\rm gauge}_{\rm 5d}$ and $\mathscr{L}^{\rm fermion}_{\rm 5d}$ are governed by the gauge principle and $V_{\rm eff}(\theta_H)$ follows from them.

3. Gauge couplings and Higgs couplings

Let us focus on the A-model. The SM quark-lepton content is reproduced with no exotic light fermions. The one-loop effective potential $V_{\rm eff}(\theta_H)$ is displayed by in fig. 1. The finite Higgs boson mass $m_H \sim 125\,{\rm GeV}$ is generated naturally with $\theta_H \sim 0.1$. Relevant parameters in the theory are determined from quark-lepton masses, m_Z, and electromagnetic, weak, and strong gauge coupling constants. Many of physical quantities depend on the value of θ_H, but not on other parameters. In the SM the W and Z couplings of quarks and leptons are universal. They depend on only representations of the group $SU(2)_L \times U(1)_Y$. In GHU the W and Z couplings of quarks and leptons may depend on more detailed behavior of wave functions in the fifth dimension. Four-dimensional couplings are obtained by integrating the product of the W/Z and quark/lepton wave functions over the fifth dimensional coordinate.

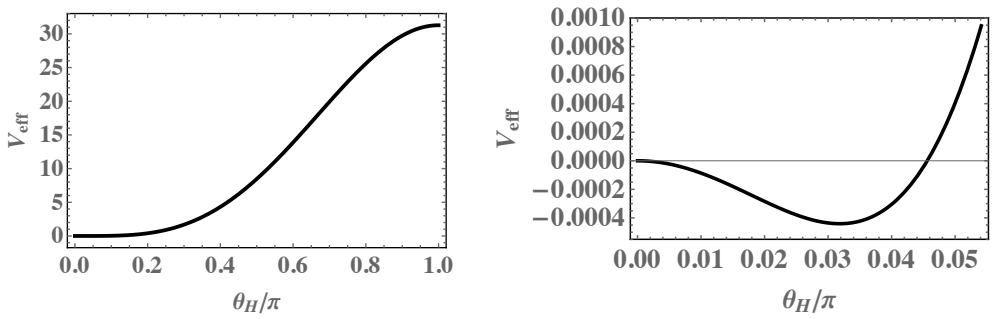

Figure 1: Effective potential $V_{\rm eff}(\theta_H)$ is displayed in the unit of $(kz_L^{-1})^4/16\pi^2$ for $z_L = 3.56\times 10^4$ and $m_{\rm KK} = 8.144\,{\rm TeV}$. The minimum of $V_{\rm eff}$ is located at $\theta_H = 0.10$. The curvature at the minimum determines the Higgs boson mass by $m_H^2 = f_H^{-2} V''_{\rm eff}(\theta_H)|_{\rm min}$, yielding $m_H = 125.1\,{\rm GeV}$.

Surprisingly the W and Z couplings of quarks and leptons and the WWZ coupling in GHU turn out very close to those in the SM. The result is tabulated in Table 2. In the last column the values in the SM are listed. The deviations from the SM are very small. The W couplings of left-handed light quarks and leptons are approximately given by

$$g_L^W \sim g_w \frac{\sqrt{2kL}}{\sqrt{2kL - \frac{3}{4}\sin^2\theta_H}} \sim g_w \left(1 + \frac{3\sin^2\theta_H}{16kL}\right). \tag{3.1}$$

Here $kL = \ln z_L$. The W couplings of right-handed quarks and leptons are negligibly small.

Yukawa couplings of quarks and leptons, and WWH, ZZH couplings are well approximated by

$$\begin{pmatrix} g_{\rm Yukawa} \\ g_{WWH} \\ g_{ZZH} \end{pmatrix} \sim \begin{pmatrix} g^{\rm SM}_{\rm Yukawa} \\ g^{\rm SM}_{WWH} \\ g^{\rm SM}_{ZZH} \end{pmatrix} \times \cos\theta_H \tag{3.2}$$

Table 2: Gauge (W,Z) couplings of quarks and leptons. WWZ coupling is also listed at the bottom. The values in the SM are listed in the last column.

		$\theta_H = 0.115$		$\theta_H = 0.0737$		SM	
g_L^W/g_w	(ν_e, e)	1.00019		1.00009		1	
	(ν_μ, μ)	1.00019		1.00009			
	(ν_τ, τ)	1.00019		1.00009			
	(u,d)	1.00019		1.00009		1	
	(c,s)	1.00019		1.00009			
	(t,b)	0.9993		0.9995			
$(g_L^Z, g_R^Z)/g_w$	ν_e, ν_μ, ν_τ	0.50014	0	0.50008	0	0.5	0
	e, μ, τ	-0.2688	0.2314	-0.2688	0.2313	-0.2688	0.2312
	u, c	0.3459	-0.1543	0.3459	-0.1542	0.3458	-0.1541
	t	0.3449	-0.1553	0.3453	-0.1549		
	d, s	-0.4230	0.0771	-0.4230	0.0771	-0.4229	0.0771
	b	-0.4231	0.0771	-0.4230	0.0771		
$g_{WWZ}/g_w \cos\theta_W$		0.9999998		0.99999995		1	

where $g^{\rm SM}_{\rm Yukawa}$ on the right side, for instance, denotes the value in the SM. For $\theta_H \sim 0.1$ the deviation amounts to only 0.5%. Larger deviations are expected in the cubic and quartic self-couplings of the Higgs boson. They are approximately given by

$$\lambda_3^{\rm Higgs} \sim 156.9\cos\theta_H + 17.6\cos^2\theta_H \ \ ({\rm GeV}),$$
$$\lambda_4^{\rm Higgs} \sim -0.257 + 0.723\cos 2\theta_H + 0.040\cos 4\theta_H \ . \tag{3.3}$$

In the SM, $\lambda_3^{\rm Higgs,SM} = 190.7\,{\rm GeV}$ and $\lambda_4^{\rm Higgs,SM} = 0.774$. In the $\theta_H \to 0$ limit $\lambda_3^{\rm Higgs}$ and $\lambda_4^{\rm Higgs}$ become 8.5% and 35% smaller than the values in the SM. $\lambda_3^{\rm Higgs}$ can be measured at ILC.

GHU gives nearly the same phenomenology at low energies as the SM. To distinguish GHU from the SM, one need to look at signals of new particles which GHU predicts.

4. New particles – KK excitation

KK excitations of each particle appear as new particles. The existence of an extra dimension is confirmed by observing KK excited particles of quarks, leptons, and gauge bosons. The KK spectrum is shown in Table 3. Z_R is the gauge field associated with $SU(2)_R$, and has no zero mode. $Z^{(1)}$, $\gamma^{(1)}$ and $Z_R^{(1)}$ are called as Z' bosons. Clean signals can be found in the process $q\bar{q} \to Z' \to e^+e^-, \mu^+\mu^-$ at LHC. So far no event of Z' has been observed, which puts the limit $\theta_H < 0.11$.

The KK mass scale as a function of θ_H is approximately given by

$$m_{\rm KK}(\theta_H) \sim \frac{1.36\,{\rm TeV}}{(\sin\theta_H)^{0.778}} \ , \tag{4.1}$$

Table 3: The mass spectrum $\{m_n\}$ $(n \geq 1)$ of KK excited modes of gauge bosons and quarks for $\theta_H = 0.10, n_F = 4$, where n_F is the number of dark fermion multiplets. Masses are given in the unit of TeV. Pairs $(W^{(n)}, Z^{(n)})$, $(W_R^{(n)}, Z_R^{(n)})$, $(t^{(n)}, b^{(n)})$, $(c^{(n)}, s^{(n)})$, $(u^{(n)}, d^{(n)})$ $(n \geq 1)$ have almost degenerate masses. The spectrum of W_R tower is the same as that of Z_R tower. The gluon tower has the same spectrum as the photon (γ) tower.

$\theta_H = 0.10,\ n_F = 4,\ m_{\rm KK} = 8.144\,{\rm TeV},\ z_L = 3.56 \times 10^4$								
	$Z^{(n)}$		$\gamma^{(\ell)}$	$Z_R^{(\ell)}$	$t^{(n)}$		$c^{(n)}$	$u^{(n)}$
$n\,(\ell)$	m_n	$\frac{m_n}{m_{\rm KK}}$	m_ℓ	m_ℓ	m_n	$\frac{m_n}{m_{\rm KK}}$	m_n	m_n
$1\,(1)$	6.642	0.816	6.644	6.234	7.462	0.916	8.536	10.47
2	9.935	1.220	–	–	8.814	1.082	12.01	13.82
$3\,(2)$	14.76	1.812	14.76	14.31	15.58	1.913	16.70	18.76
4	18.19	2.233	–	–	16.99	2.087	20.41	22.37

irrespective of the other parameters of the theory. In GHU many of physical quantities such as the Higgs couplings in (3.2) and (3.3), the KK scale (4.1), and KK masses of gauge bosons are approximately determined by the value of θ_H only. This property is called as the θ_H universality. Once the $Z^{(1)}$ particle is found and its mass is determined, then the value of θ_H is fixed and the values of other physical quantities are predicted.[8]

Although Z' bosons are heavy with masses around 6 – 8 TeV, their effects can be seen at 250 GeV ILC (e^+e^- collisions). (Fig. 2) The couplings of right-handed quarks and leptons to Z' bosons are much stronger than those of left-handed quarks and leptons. This large parity violation manifests as an interference effect in e^+e^- collisions.[11]

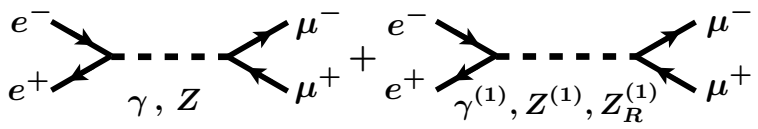

Figure 2: Dominant diagrams in the process $e^+e^- \to \mu^+\mu^-$

Left-handed light quarks and leptons are localized near the UV brane (at $y = 0$), whereas right-handed ones near the IR brane (at $y = L$). Wave functions of top and bottom quarks spread over the entire fifth dimension. In GHU both left- and right-handed fermions are in the same gauge multiplet so that if a left-handed fermion is localized near the UV brane, then its partner right-handed fermion is necessarily localized near the IR brane. KK modes of gauge bosons in the RS space are always localized near the IR brane. Z' couplings of quarks and leptons are given by overlap-integrals of wave functions of Z' bosons and left- or right-handed quarks and leptons. Consequently right-handed quarks/leptons have larger couplings to Z'. Typical behavior of wave functions is depicted in fig. 3.

Gauge couplings of quarks and leptons to $Z^{(1)}$, $\gamma^{(1)}$ and $Z_R^{(1)}$ are summarized in Table 4. Except for b and t quarks, right-handed quarks and leptons have much larger couplings than left-handed ones.

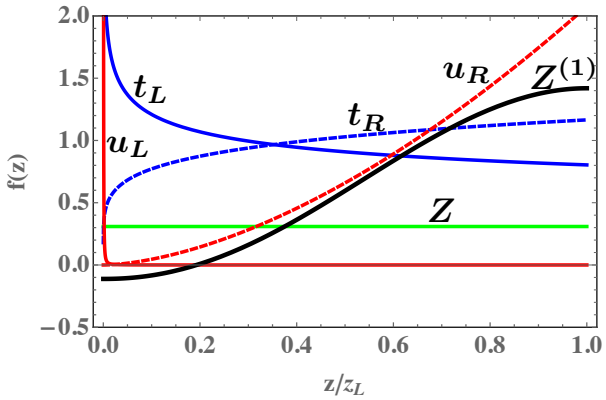

Figure 3: Wave functions of various fermions and gauge bosons for $\theta_H = 0.1$. Only some of the relevant components in $SO(5)$ are displayed. Wave functions of light quarks and leptons are qualitatively similar to those of (u_L, u_R). Wave functions of (b_L, b_R) are similar to those of (t_L, t_R). Z boson wave function is almost constant, whereas $Z^{(1)}$'s wave function becomes large near the IR brane at $z = z_L$.

Table 4: Gauge couplings of quarks and leptons to $Z^{(1)}$, $\gamma^{(1)}$ and $Z_R^{(1)}$ for $\theta_H = 0.0917$ and $\sin^2\theta_W = 0.2312$. Couplings are given in the unit of $g_w/\cos\theta_W$. The Z couplings in the SM , $I_3 - \sin^2\theta_W Q_{\rm EM}$, are also shown.

	SM: Z		$Z^{(1)}$		$Z_R^{(1)}$		$\gamma^{(1)}$	
	Left	Right	Left	Right	Left	Right	Left	Right
ν_e			−0.183	0	0	0	0	0
ν_μ	0.5	0	−0.183	0	0	0	0	0
ν_τ			−0.183	0	0	0	0	0
e			0.099	0.916	0	−1.261	0.155	−1.665
μ	−0.269	0.231	0.099	0.860	0	−1.193	0.155	−1.563
τ			0.099	0.814	0	−1.136	0.155	−1.479
u			−0.127	−0.600	0	0.828	−0.103	1.090
c	0.346	−0.154	−0.130	−0.555	0	0.773	−0.103	1.009
t			0.494	−0.372	0.985	0.549	0.404	0.678
d			0.155	0.300	0	−0.414	0.052	−0.545
s	−0.423	0.077	0.155	0.277	0	−0.387	0.052	−0.504
b			−0.610	0.186	0.984	−0.274	−0.202	−0.339

5. e^+e^- collisions

The amplitude $\mathscr{M}$ for the $e^+e^- \to \mu^+\mu^-$ process at the tree level in fig. 2 can be expressed as the sum of two terms $\mathscr{M}_0$ and $\mathscr{M}_{Z'}$.

$$\begin{aligned}\mathscr{M} &= \mathscr{M}_0 + \mathscr{M}_{Z'} \\ &= \mathscr{M}(e^+e^- \to \gamma, Z \to \mu^+\mu^-) + \mathscr{M}(e^+e^- \to Z' \to \mu^+\mu^-)\,. \end{aligned} \tag{5.1}$$

For $s = (250\,\text{GeV})^2 \sim (1\,\text{TeV})^2$, we have $m_Z^2 \ll s \ll m_{Z'}^2$ so that the amplitude can be approximated

by

$$\mathscr{M} \simeq \frac{g_w^2}{\cos^2\theta_W} \sum_{\alpha,\beta=L,R} J_\alpha^{(e)\nu}(p,p') \left\{ \frac{\kappa_{\rm SM}^{\alpha\beta}}{s} - \frac{\kappa_{Z'}^{\alpha\beta}}{m_{Z'}^2} \right\} J_{\beta\nu}^{(\mu)}(k,k') \tag{5.2}$$

where $J_{\alpha\nu}^{(e)}(p,p')$ and $J_{\beta\nu}^{(\mu)}(k,k')$ represent momentum and polarization configurations of the initial and final states, respectively. $\kappa_{\rm SM}^{\alpha\beta}$ and $\kappa_{Z'}^{\alpha\beta}$ are found from Table 4 to be

$$\begin{aligned} (\kappa_{\rm SM}^{LL}, \kappa_{\rm SM}^{LR}, \kappa_{\rm SM}^{RL}, \kappa_{\rm SM}^{RR}) &= (0.25, 0.1156, 0.1156, 0.2312)\ , \\ (\kappa_{Z'}^{LL}, \kappa_{Z'}^{LR}, \kappa_{Z'}^{RL}, \kappa_{Z'}^{RR}) &= (0.034, -0.158, -0.168, 4.895)\ . \end{aligned} \tag{5.3}$$

Compared with the value in the SM, $\kappa_{Z'}^{RR}$ is very large whereas $\kappa_{Z'}^{LL}$ is very small.

Although direct production of Z' particles is not possible with $s = (250\,\text{GeV})^2 \sim (1\,\text{TeV})^2$, the interference term becomes appreciable. Suppose that the electron beam is polarized in the right-handed mode. Then the interference term gives

$$\begin{aligned} \frac{\mathscr{M}_0 \mathscr{M}_{Z'}^*}{|\mathscr{M}_0|^2} &\sim -\frac{\kappa_{Z'}^{RR} + \kappa_{Z'}^{RL}}{\kappa_{\rm SM}^{RR} + \kappa_{\rm SM}^{RL}} \frac{s}{m_{Z'}^2} \sim -13.6 \frac{s}{m_{Z'}^2} \\ &\sim -0.017 \quad \text{at } \sqrt{s} = 250\,\text{GeV}\ . \end{aligned} \tag{5.4}$$

This is a sufficiently big number. As the number of events of fermion pair production is huge in the proposed ILC experiment, 1.7% correction can be certainly confirmed. One recognizes that polarized electron and/or positron beams play an important role to investigate physics beyond the SM.[11], [12], [22]-[25]

5.1 Energy and polarization dependence

In the e^+e^- collision experiments one can control both the energy and polarization of incident electron and positron beams. First consider the total cross section for $e^+e^- \to \mu^+\mu^-$;

$$F_1 = \frac{\sigma(e^+e^- \to \mu^+\mu^-)^{\rm GHU}}{\sigma(e^+e^- \to \mu^+\mu^-)^{\rm SM}}\ . \tag{5.5}$$

Both the electron and positron beams are polarized with polarization P_{e^-} and P_{e^+}. For purely right-handed (left-handed) electrons $P_{e^-} = +1(-1)$. At $\sqrt{s} \geq 250\,\text{GeV}$, e^+ and e^- in the initial state may be viewed as massless particles. The ratio F_1 in (5.5) depends on the effective polarization

$$P_{\rm eff} = \frac{P_{e^-} - P_{e^+}}{1 - P_{e^-}P_{e^+}}\ . \tag{5.6}$$

At the proposed 250 GeV ILC, $|P_{e^-}| \leq 0.8$ and $|P_{e^+}| \leq 0.3$ so that $|P_{\rm eff}| \leq 0.877$.

The $\sqrt{s}$ dependence of F_1 is depicted in fig. 4 (a). The deviation from the SM becomes very large at $\sqrt{s} = 1.5\,\text{TeV} \sim 2\,\text{TeV}$ for $\theta_H = 0.09 \sim 0.07$, particularly with $P_{\rm eff} \sim 0.8$. For $P_{\rm eff} \sim -0.8$ the deviation is tiny. At the energy $\sqrt{s} = 250\,\text{GeV}$ the deviation might look small. As the event number expected at ILC is so huge that deviation can be unambiguously observed even at $\sqrt{s} = 250\,\text{GeV}$. In fig. 4 (b) the polarization $P_{\rm eff}$ dependence of F_1 is depicted for $\sqrt{s} = 250\,\text{GeV}$

and 500 GeV. As the polarization $P_{\rm eff}$ varies from -1 to $+1$, deviation from the SM becomes significantly larger. The grey band in fig. 4 (b) indicates statistical uncertainty at $\sqrt{s} = 250\,\text{GeV}$ with $250\,\text{fb}^{-1}$ data set in the SM. It is seen that the signal of GHU can be clearly seen by measuring the polarization dependence in the early stage of ILC 250 GeV.

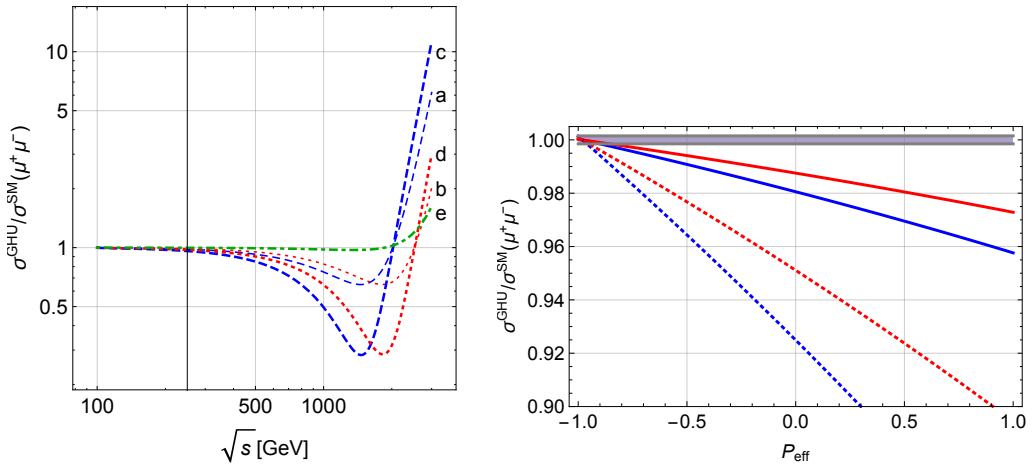

(a) (b)

Figure 4: $F_1 = \sigma(\mu^+\mu^-)^{\rm GHU}/\sigma(\mu^+\mu^-)^{\rm SM}$ in (5.5) is plotted. (a) The $\sqrt{s}$ dependence is shown. Blue curves a, c and green curve e are for $\theta_H = 0.0917$, whereas red curves b, d are for $\theta_H = 0.0737$. Curves a and b are with $P_{\rm eff} = 0$. Curves c and d are with $P_{\rm eff} = 0.877$. Curve e is with $P_{\rm eff} = -0.877$. (b) The polarization $P_{\rm eff}$ dependence is shown. Solid (dashed) lines are for $\sqrt{s} = 250\,\text{GeV}$ (500 GeV). Blue lines are for $\theta_H = 0.0917$, whereas red lines are for $\theta_H = 0.0737$. The grey band indicates statistical uncertainty at $\sqrt{s} = 250\,\text{GeV}$ with $250\,\text{fb}^{-1}$ data set.

5.2 Forward-backward asymmetry

Not only in the total cross sections but also in differential cross sections for $e^+e^- \to \mu^+\mu^-$ significant deviation from the SM can be seen.[23, 24] Even with unpolarized beams the differential cross sections $d\sigma/d\cos\theta$ becomes 8% (4%) smaller than in the SM in the forward direction for $\theta_H = 0.0917$ (0.0737).

Forward-backward asymmetry $A_{\rm FB}$ characterizes this behavior. In fig. 5(a) the $\sqrt{s}$-dependence of $A_{\rm FB}$ for $e^+e^- \to \mu^+\mu^-$ is shown. As $\sqrt{s}$ increases the deviation from the SM becomes evident. Again the deviation becomes largest around $\sqrt{s} = 1.5 \sim 2\,\text{TeV}$ with $P_{\rm eff} = 0.877$ for $\theta_H = 0.0917 \sim 0.0737$. The sign of $A_{\rm FB}$ flips around $\sqrt{s} = 1.1 \sim 1.5\,\text{TeV}$.

Even at $\sqrt{s} = 250\,\text{GeV}$, significant deviation from the SM can be seen in the dependence on the polarization ($P_{\rm eff}$) of the electron/positron beam as depicted in fig. 5(b). With $250\,\text{fb}^{-1}$ data the deviation amounts to 6σ (4σ) at $P_{\rm eff} = 0.8$ for $\theta_H = 0.0917\,(0.0737)$, whereas the deviation is within an error at $P_{\rm eff} = -0.8$. Observing the polarization dependence is a definitive way of investigating the details of the theory.

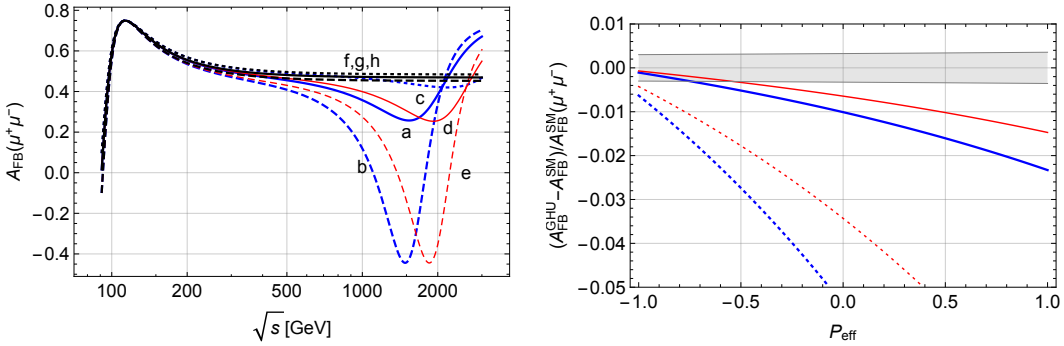

(a) (b)

Figure 5: Forward-backward asymmetry $A_{\rm FB}(\mu^+\mu^-)$. (a) The $\sqrt{s}$ dependence is shown. Blue curves a, b, c are for $\theta_H = 0.0917$, red curves d, e are for $\theta_H = 0.0737$, and black curves f, g, h are for the SM. Solid curves a, d, f are for unpolarized beams. Dashed curves b, e, g are with $P_{\rm eff} = 0.877$. Dotted curves c and h are with $P_{\rm eff} = -0.877$. (b) $(A_{\rm FB}^{\rm GHU} - A_{\rm FB}^{\rm SM})/A_{\rm FB}^{\rm SM}(\mu^+\mu^-)$ as functions of the effective polarization $P_{\rm eff}$. Solid and dotted lines are for $\sqrt{s} = 250\,$GeV and 500 GeV, respectively. Blue and red lines correspond to $\theta_H = 0.0917$ and 0.0737, respectively. The gray band indicates the statistical uncertainty at $\sqrt{s} = 250\,$GeV with 250 fb^{-1} data.

5.3 Left-right asymmetry

Systematic errors in the normalization of the cross sections are reduced in the measurement of

$$R_{f,LR}(\overline{P}) = \frac{\sigma(\bar{f}f; P_{e^-} = +\overline{P}, P_{e^+} = 0)}{\sigma(\bar{f}f; P_{e^-} = -\overline{P}, P_{e^+} = 0)} \tag{5.7}$$

where the electron beams are polarized with $P_{e^-} = +\overline{P}$ and $-\overline{P}$. Only the polarization of the electron beams is flipped in experiments. Let σ_{LR}^f (σ_{RL}^f) denote the $e_L^- e_R^+ (e_R^- e_L^+) \to f\bar{f}$ scattering cross section. Then the left-right asymmetry A_{LR}^f is related to $R_{f,LR}$ by

$$A_{LR}^f = \frac{\sigma_{LR}^f - \sigma_{RL}^f}{\sigma_{LR}^f + \sigma_{RL}^f} = \frac{1}{\overline{P}} \frac{1 - R_{f,LR}}{1 + R_{f,LR}} \,. \tag{5.8}$$

The predicted $R_{f,LR}(\overline{P})$ is summarized in Table 5 for $\overline{P} = 0.8$. Even at $\sqrt{s} = 250\,$GeV with $L_{int} = 250\,$fb^{-1} data, namely in the early stage of the ILC experiment, significant deviation from the SM is seen. The difference between $R_{\mu,LR}$ and $R_{b,LR}$ stems from the different behavior of wave functions of μ and b in the fifth dimension.

6. Summary

Gauge-Higgs unification predicts large parity violation in the quark-lepton couplings to the Z' bosons ($Z^{(1)}, \gamma^{(1)}, Z_R^{(1)}$). Although these Z' bosons are very heavy with masses 7 - 8 TeV, they give rise to significant interference effects in e^+e^- collisions at $\sqrt{s} = 250\,$GeV $\sim 1\,$TeV. We examined the A-model of $SO(5) \times U(1) \times SU(3)$ gauge-Higgs unification, and found that significant deviation can be seen at 250 GeV ILC with 250 fb^{-1} data. Polarized electron and positron beams are

Table 5: $R_{f,LR}(\overline{P})$ in the SM, and deviations of $R_{f,LR}(\overline{P})^{\rm GHU}/R_{f,LR}(\overline{P})^{\rm SM}$ from unity are tabulated for $\overline{P}=0.8$. Statistical uncertainties of $R^{\rm SM}_{f,LR}$ is estimated with L_{int} data for both $\sigma(\bar{f}f;P_{e^-}=+\overline{P})$ and $\sigma(\bar{f}f;P_{e^-}=-\overline{P})$, namely with $2L_{int}$ data in all.

f	$\sqrt{s}$, L_{int}	SM	GHU	
		$R^{SM}_{f,LR}$ (uncertainty)	$\theta_H=0.0917$	$\theta_H=0.0737$
μ	250 GeV, 250 fb^{-1}	0.890 (0.3%)	-3.4%	-2.2%
	500 GeV, 500 fb^{-1}	0.900 (0.4%)	-13.2%	-8.6%
b	250 GeV, 250 fb^{-1}	0.349 (0.3%)	-3.1%	-2.1%
	500 GeV, 500 fb^{-1}	0.340 (0.5%)	-12.3%	-8.3%
t	500 GeV, 500 fb^{-1}	0.544 (0.4%)	-13.0%	-8.2%

indispensable. All of the total cross section, differential cross section, forward-backward asymmetry, and left-right asymmetry for $e^+e^-\to f\bar{f}$ processes show distinct dependence on the energy and polarization.

We stress that new particles of masses 7 - 8 TeV can be explored at 250 GeV ILC by seeing the interference effect, but not by direct production. This is possible at e^+e^- colliders because the number of $e^+e^-\to f\bar{f}$ events is huge. Although the probability of directly producing Z' bosons is suppressed by a factor $(s/m^2_{Z'})^2$, the interference term is suppressed only by a factor of $s/m^2_{Z'}$. This gives a big advantage over pp colliders such as LHC.

In this talk the predictions coming from the A-model are presented. It is curious to see how predictions change in the B-model. Preliminary study indicates the pattern of the polarization dependence is reversed in the B-model in comparison with the A-model. The B-model is motivated by the idea of grand unification, which, in my opinion, is absolute necessity in GHU in the ultimate form. The A-model cannot be implemented in natural grand unification. Satisfactory grand unification in GHU has not been achieved yet.[19, 20, 21], [26]-[32]

There are many other issues to be solved in GHU. Mixing in the flavor sector, behavior at finite temperature, inflation in cosmology, and baryon number generation are among them. I would like to come back to these issues in due course.

Acknowledgement

This work was supported in part by Japan Society for the Promotion of Science, Grants-in-Aid for Scientific Research, No. 15K05052 and No. 19K03873.

References

[1] Y. Hosotani, *"Dynamical mass generation by compact extra dimensions"*, *Phys. Lett.* B**126**, 309 (1983); *"Dynamics of nonintegrable phases and gauge symmetry breaking"*, *Ann. Phys. (N.Y.)* **190**, 233 (1989).

[2] A. T. Davies and A. McLachlan, *"Gauge group breaking by Wilson loops"*, *Phys. Lett.* B**200**, 305 (1988); *"Congruency class effects in the Hosotani model"*, *Nucl. Phys.* B**317**, 237 (1989).

[3] H. Hatanaka, T. Inami, C.S. Lim, *"The Gauge hierarchy problem and higher dimensional gauge theories"*, *Mod. Phys. Lett.* A**13**, 2601 (1998).

[4] M. Kubo, C.S. Lim and H. Yamashita, *"The Hosotani mechanism in bulk gauge theories with an orbifold extra space S^1/Z_2"*, *Mod. Phys. Lett.* A**17**, 2249 (2002).

[5] K. Agashe, R. Contino and A. Pomarol, *"The minimal composite Higgs model"*, *Nucl. Phys.* B**719**, 165 (2005).

[6] A. D. Medina, N. R. Shah and C. E. M. Wagner, *"Gauge-Higgs unification and radiative electroweak symmetry breaking in warped extra dimensions"*, *Phys. Rev.* D**76**, 095010 (2007).

[7] Y. Hosotani, K. Oda, T. Ohnuma and Y. Sakamura, *"Dynamical electroweak symmetry breaking in $SO(5)\times U(1)$ gauge-Higgs unification with top and bottom quarks"*, *Phys. Rev.* D**78**, 096002 (2008); *Erratum-ibid.* D**79**, 079902 (2009).

[8] S. Funatsu, H. Hatanaka, Y. Hosotani, Y. Orikasa and T. Shimotani, *"Novel universality and Higgs decay $H\to\gamma\gamma, gg$ in the $SO(5)\times U(1)$ gauge-Higgs unification"*, *Phys. Lett.* B**722**, 94 (2013).

[9] S. Funatsu, H. Hatanaka, Y. Hosotani, Y. Orikasa, and T. Shimotani, *"LHC signals of the $SO(5)\times U(1)$ gauge-Higgs unification"*, *Phys. Rev.* D**89**, 095019 (2014).

[10] S. Funatsu, H. Hatanaka, Y. Hosotani and Y. Orikasa, *"Collider signals of W' and Z' bosons in the gauge-Higgs unification"*, *Phys. Rev.* D**95**, 035032 (2017).

[11] S. Funatsu, H. Hatanaka, Y. Hosotani and Y. Orikasa, *"Distinct signals of the gauge-Higgs unification in e^+e^- collider experiments"*, *Phys. Lett.* B**775**, 297 (2017).

[12] J. Yoon and M.E. Peskin, *"Dissection of an $SO(5)\times U(1)$ gauge-Higgs unification model"*, arXiv:1810.12352; *"Fermion pair production in $SO(5)\times U(1)$ gauge-Higgs unification models"*, arXiv:1811.07877.

[13] S. Funatsu, H. Hatanaka, Y. Hosotani, Y. Orikasa, and N. Yamatsu, *"GUT inspired $SO(5)\times U(1)\times SU(3)$ gauge-Higgs unification"*, arXiv:1902.01603, to appear in *Phys. Rev.* D.

[14] S. Funatsu, H. Hatanaka, Y. Hosotani, Y. Orikasa and T. Shimotani, *"Dark matter in the $SO(5)\times U(1)$ gauge-Higgs unification"*, *Prog. Theoret. Exp. Phys.* **2014**, 113B01 (2014).

[15] N. Maru, N. Okada and S. Okada, *"$SU(2)_L$ doublet vector dark matter from gauge-Higgs unification"*, *Phys. Rev.* D**98**, 075021 (2018).

[16] Y. Adachi and N. Maru, *"Revisiting electroweak symmetry breaking and the Higgs boson mass in gauge-Higgs unification"*, *Phys. Rev.* D**98**, 015022 (2018).

[17] K. Hasegawa and C.S. Lim, *"Majorana neutrino masses in the scenario of gauge-Higgs unification"*, *Prog. Theoret. Exp. Phys.* **2018**, 073B01 (2018).

[18] C.S. Lim, *"The implication of gauge-Higgs unification for the hierarchical fermion masses"*, *Prog. Theoret. Exp. Phys.* **2018**, 093B02 (2018).

[19] Y. Hosotani and N. Yamatsu, *"Gauge-Higgs grand unification"*, *Prog. Theoret. Exp. Phys.* **2015**, 111B01 (2015).

[20] A. Furui, Y. Hosotani, and N. Yamatsu, *"Toward realistic gauge-Higgs grand unification"*, *Prog. Theoret. Exp. Phys.* **2016**, 093B01 (2016).

[21] Y. Hosotani and N. Yamatsu, *"Gauge-Higgs seesaw mechanism in 6-dimensional grand unification"*, *Prog. Theoret. Exp. Phys.* **2017**, 091B01 (2017).

[22] S. Bilokin, R. Poschl and F. Richard, *"Measurement of b quark EW couplings at ILC"*, arXiv:1709.04289 [hep-ex].

[23] F. Richard, *"Bhabha scattering at ILC250"*, arXiv:1804.02846 [hep-ex].

[24] T. Suehara, in presentation *"Precise measurement of two-fermion final states in 250 GeV ILC for*

BSM", at Asian Linear Collider Workshop 2018, (Fukuoka, 2018).

[25] ILC Collaboration (H. Aihara et al.), *"The International Linear Collider. A global project"*, arXiv:1901.09829 [hep-ex]; Philip Bambade et al.. *"The International Linear Collider. A global project"*, arXiv:1903.01629 [hep-ex].

[26] G. Burdman and Y. Nomura, *"Unification of Higgs and gauge fields in five dimensions"*, *Nucl. Phys.* B**656**, 3 (2003).

[27] N. Haba, Masatomi Harada, Y. Hosotani and Y. Kawamura, *"Dynamical rearrangement of gauge symmetry on the orbifold S^1/Z_2"*, *Nucl. Phys.* B**657**, 169 (2003); *Erratum-ibid.* B**669**, 381 (2003).

[28] N. Haba, Y. Hosotani, Y. Kawamura and T. Yamashita, *"Dynamical symmetry breaking in gauge-Higgs unification on orbifold"*, *Phys. Rev.* D**70**, 015010 (2004).

[29] C.S. Lim and N. Maru, *"Towards a realistic grand gauge-Higgs unification"*, *Phys. Lett.* B**653**, 320 (2007).

[30] K. Kojima, K. Takenaga and T. Yamashita, *"Grand gauge-Higgs unification"*, *Phys. Rev.* D**84**, 051701(R) (2011); *"Gauge symmetry breaking patterns in an SU(5) grand gauge-Higgs unification"*, *Phys. Rev.* D**95**, 015021 (2017).

[31] M. Frigerio, J. Serra and A. Varagnolo, *"Composite GUTs: models and expectations at the LHC"*, *JHEP* **1106**, 029 (2011).

[32] N. Maru and Y. Yatagai, *"Fermion mass hierarchy in grand gauge-Higgs unification"*, arXiv:1903.08359.